Journal of Applied Engineering Mathematics

Volume 8, December 2021

MODELING 2-DIMENSIONAL HYDROGEN DIFFUSION USING FICK'S 2ND LAW

Jeremy Green

Mechanical Engineering Department
Brigham Young University
Provo, Utah 84602
jgreen43@byu.edu

ABSTRACT

Hydrogen diffusion is believed to be one of the main mechanisms through which hydrogen enters a material and degrades its properties. By better understanding this process, materials resistant to hydrogen embrittlement can be produced. In this work, a 2-dimensional model of hydrogen diffusion through a uniform cross section material is constructed using Fick's 2nd Law. Various concentration surface conditions are considered. For the Neuman-Dirichlet boundary condition hydrogen largely remains close to the surface of the sample and a majority of the sample only experiences a small increase in concentration.

NOMENCLATURE

- c: Concentration
- D: Diffusion Coefficient
- x: Thickness Variable
- y: Height Variable
- GB: Grain Boundary
- TJ: Triple Junction

INTRODUCTION

Diffusion is a method of a molecular transport where small particles move through another material medium due to a concentration gradient. In this analysis, studies on hydrogen diffusion through nickel will be used as the basis for discussion and modelling.

Metals are composed of smaller crystal units known as grains. Each grain is composed of an atomic lattice following a prescribed packing order (FCC for nickel). Diffusion occurs when hydrogen atoms move to locations that are more energetically favorable both in and around grains. Hydrogen preferentially migrates to locations such as sites in planes with lower atomic packing [1] or areas with lower internal stresses [2].

The grains and the interaction between grains influences diffusion. Interfaces between two grains known as GBs have been seen to directly influence diffusion. GBs of various types and orientations can acts as hydrogen traps or accelerators [3] [4] [5] [6]. Additionally, interfaces between three grains known as triple junctions (TJs) act as superconductors for hydrogen diffusion [7] [8]. These all-cause anisotropy of diffusion on a microstructural level. Further, it has been shown that hydrogen diffusion through single crystal nickel is anisotropic in nature [2].

While diffusion occurs anisotropically on a microstructural scale, generally it occurs isotopically on a macrostructural scale. This is due to the fact that averaging randomly sized and oriented grains over large grain counts, tends to produce general patterns. Representative and statistical volume elements define how many grains are required to give an accurate representation of these properties for the bulk material.

The constructed model is based on the assumption that diffusion behaves isotopically. Fick's Laws and the other tools used to model diffusion would need to be modified to account for directional diffusion in very small samples.

METHODS

1. Experimental Procedures

The model was built based on the ASTM standards for electrochemically measuring hydrogen diffusion through a material [9]. The setup involves two chambers known as Devanathan cells. Each cell has an identical hole or opening where a material sample is clamped between the two cells. Aqueous sodium hydroxide or another strong electrolyte is added to both cells such that the fluid and material interface keeps the fluid from leaking. The area of the sample exposed to the fluid is where hydrogen can diffuse through the material and transfer between cells.

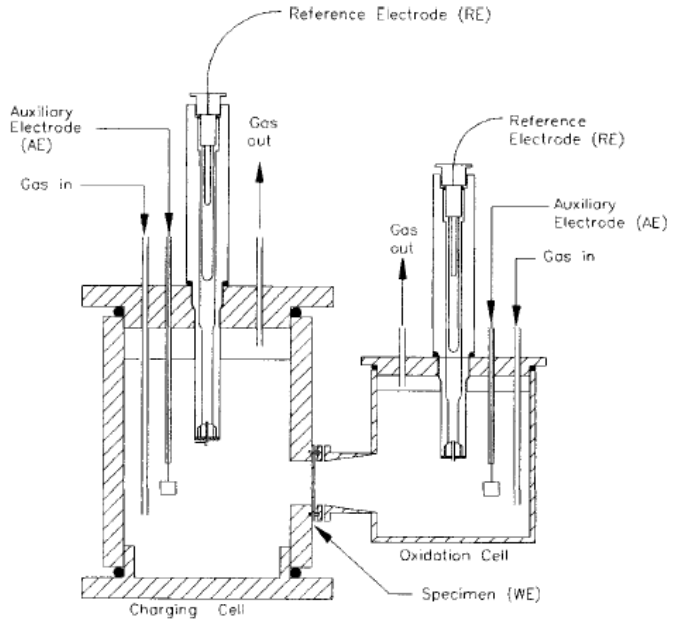

Figure 1: Diagram of the experimental setup used as the foundation of the model. [9]

Each cell is connected to a potentiostat to regulate the voltage applied to the system. Reference and auxiliary electrodes are inserted into the fluid while a working electrode is connected directly to the sample. By running electricity through a cell, it causes the hydrogen ions to disassociate. In this state they are positively charged which draws them toward the electrode acting as the anode. Depending on which way the voltage is applied this can be either the sample or auxiliary electrode. Effectively this allows the hydrogen concentration gradient to be controlled, either massing hydrogen by the sample or by an electrode far from the sample.

Prior to an experiment, both potentiostats are configured to draw hydrogen toward the auxiliary electrode in a pre-charge. This creates a low concentration of hydrogen in the electrolyte directly next to the sample causing hydrogen to move toward and eventually exit into the nearest Devanthan cell. By doing this for a sufficient amount of time, it can be assumed that nearly all hydrogen has been removed from the sample.

Afterwards, to measure the effective diffusion of hydrogen through a sample, the current flow in one of the potentiostats is reversed. This causes hydrogen to amass near the surface of a single side of the sample. Hydrogen now diffuses through the sample as it moves from a high concentration toward a lower concentration. When it travels completely through the sample, it is drawn toward the auxiliary electrode, wicking it away from the surface thus maintaining the concentration gradient.

2. Diffusion Coefficient

Using the procedure outlined above, the effective diffusion coefficient D can be calculated as follows:

$$D = \frac{6L^2}{t_{lag}}$$

Where L is the thickness of the sample and t_{lag} is a time lag constant associated with the diffusion. It is computed as the time it takes for the current to reach 63% of its peak value as measured by the reference electrode. The increase in current is caused by the motion of the hydrogen ions. Electricity is defined as the energy associated with moving ions. Therefore, as hydrogen ions moves through the sample the current will increase as a typical 1st Order ODE until a steady state is reached. For this work it is assumed $D = 5.67 \times 10^{-14} \frac{m^2}{s}$ (compare to [2] and [3]).

3. Fick's 2nd Law

Fick's law is used to model diffusion. It is given by:

$$\frac{\partial^2 c}{\partial x^2} = \frac{1}{D}\frac{\partial c}{\partial \mathrm{t}}$$

Mathematically, it is identical to the heat equation. Modifying it for 2-dimensions yields:

$$\frac{\partial^2 c}{\partial x^2} + \frac{\partial^2 c}{\partial y^2} = \frac{1}{D}\frac{\partial c}{\partial \mathrm{t}}$$

Where x and y correspond to the thickness and the height of the sample respectively.

4. Boundary and Initial Conditions

The boundary and initial conditions of the problem are defined as follows:

$$\begin{aligned} \frac{\partial}{\partial x}c(0,y,t) &= f_0 \quad \text{Neuman} \\ c(L,y,t) &= 0 \quad \text{Dirichlet} \\ c(x,0,t) &= 0 \quad \text{Dirichlet} \\ c(x,M,t) &= 0 \quad \text{Dirichlet} \\ c(x,y,0) &= 0 \end{aligned}$$

The concentration at x = 0 will be some value described by the concentration function created by the electrodes. Under standard conditions this should be constant or the concentration gradually decreasing over time. Using a Neuman condition here signifies that no hydrogen will leave the sample through the surface that it enters in through. The wicking effect on the other side of the sample should behave as a Dirichlet condition as the hydrogen is quickly moved away producing a concentration of 0 for all time. The top and bottom edges of the sample are in contact with the air and therefore, are not anticipated to play a strong role in the diffusion interaction, especially because the height of the sample is significantly larger than the thickness.

5. Solution

Solving Fick's 2nd Law with the listed boundary and initial conditions yields.

$$c(x,y,t) = \frac{4D}{LM}\sum_{n=1}^{\infty}\sum_{m=1}^{\infty}\bar{c}_{nm}\cos(\lambda_n x)\sin(\mu_m y)$$

where:

$$\bar{c}_{nm} = \int_{\tau=0}^{\infty} -f_0(\tau)\, e^{D(\lambda_n^2+\mu_m^2)(\tau-t)}\, d\tau$$

$$\lambda_n = \left(n+\frac{1}{2}\right)\frac{\pi}{L}$$

$$\mu_m = \frac{m\pi}{M}$$

For a full derivation of the solution see Appendix A.

RESULTS

Plotting the solution yields the following visual representations. Each was approximated with 25 terms for both series. Note the powers on the x axis and color bar. See attached videos for animation to show the transient responses.

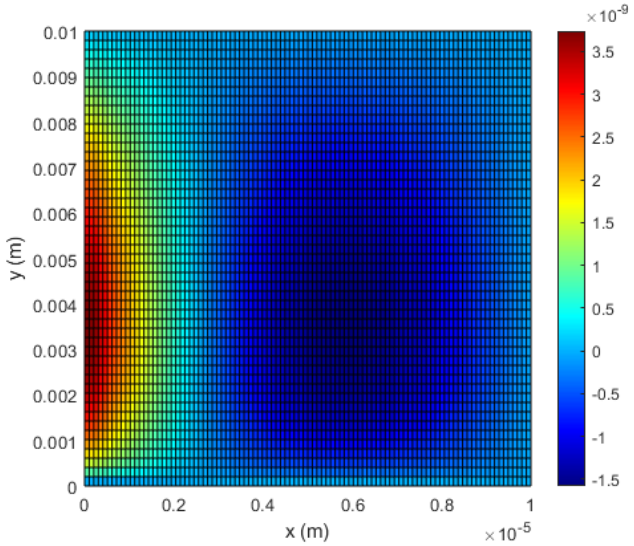

Figure 2: Concentration shown by color at steady state for a $f_0 = C$. This signifies a uniform concentration at the samples surface.

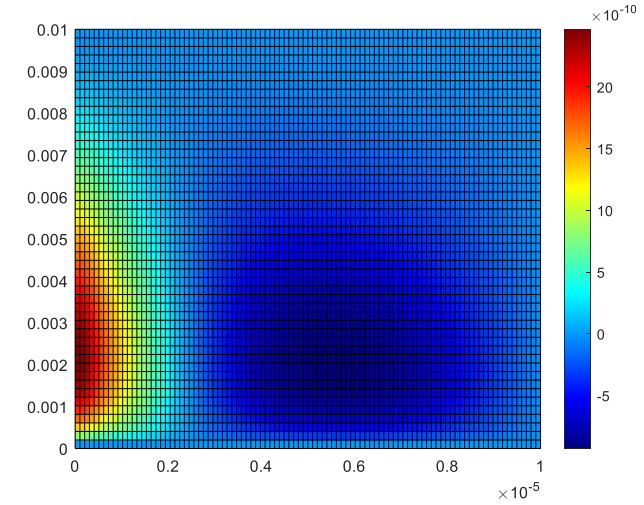

Figure 3: Concentration shown by color at steady state for a $f_0 = C - (0.01 - by)$. This signifies that the concentration of hydrogen preferentially forms towards the bottom of the sample compared to the top.

Gradually decreasing concentration gradients were also modelled ($f_0 = c - bt$). See attached videos.

As expected, these boundary conditions form circular pattern around the edge of high concentration because the upper and lower boundaries are maintained at a concentration of 0. The highly saturated region does not extend beyond the halfway point of the sample. Based on these results, pre-charging the saturated side of the sample should remove nearly all hydrogen in the sample. However, if the rate that hydrogen migrates from the low concentration side of the sample is low enough, we would expect to see an increased build-up of hydrogen within the sample. This would be modelled as a positive non-zero Dirichlet condition. It is anticipated that the regions of high concentration would expand further into the sample and overall concentration in the sample would increase.

CONCLUSIONS

Diffusion experiences a high order of exponential decay as it moves through the sample. Areas close to the high concentration experience a large uptick in concentration while the majority of the sample remains unaffected. Further investigation would be required to determine how the hydrogen would distribute when removed from the experiment. If a majority of hydrogen is irreversibly trapped, we would expect the concentration profile to remain relatively unaffected. On the other hand, if the hydrogen is still free to diffuse it would distribute itself more uniformly throughout the sample.

ACKNOWLEDGMENTS

I would like to thank my research partners Sterling Baird, Dr Oliver Johnson, and Nathan Miller for their knowledge and expertise on diffusion.

REFERENCES

[1] Torres, E., Pencer, J., & Radford, D. D. (2018). Atomistic simulation study of the hydrogen diffusion in nickel. Computational Materials Science, 152, 374-380. doi:https://doi.org/10.1016/j.commatsci.2018.06.002

[2] Li, J., Oudriss, A., Metsue, A., Bouhattate, J., & Feaugas, X. (2017). Anisotropy of hydrogen diffusion in nickel single crystals: The effects of self-stress and hydrogen concentration on diffusion. Scientific Reports, 7(1), 45041. doi:10.1038/srep45041

[3] Oudriss, A., Creus, J., Bouhattate, J., Savall, C., Peraudeau, B., & Feaugas, X. (2012a). The diffusion and trapping of hydrogen along the grain boundaries in polycrystalline nickel. Scripta Materialia, 66(1), 37-40.

doi:https://doi.org/10.1016/j.scriptamat.2011.09.036
[4] Di Stefano, D., Mrovec, M., & Elsässer, C. (2015). First-principles investigation of hydrogen trapping and diffusion at grain boundaries in nickel. Acta Materialia, 98, 306-312. doi:https://doi.org/10.1016/j.actamat.2015.07.031
[5] Ma, Z. X., Xiong, X. L., Zhang, L. N., Zhang, Z. H., Yan, Y., & Su, Y. J. (2018). Experimental study on the diffusion of hydrogen along individual grain boundaries in nickel. Electrochemistry Communications, 92, 24-28. doi:https://doi.org/10.1016/j.elecom.2018.05.012
[6] Jothi, S., Croft, T. N., & Brown, S. G. R. (2014). Influence of grain boundary misorientation on hydrogen embrittlement in bi-crystal nickel. International Journal of Hydrogen Energy, 39(35), 20671-20688. doi:https://doi.org/10.1016/j.ijhydene.2014.07.020
[7] Wang, H., Yang, W., & Ngan, A. H. W. (2005). Enhanced diffusivity by triple junction networks. Scripta Materialia, 52(1), 69-73. doi:https://doi.org/10.1016/j.scriptamat.2004.08.025
[8] Jothi, S., Croft, T. N., & Brown, S. G. R. (2015). Modelling the influence of microstructural morphology and triple junctions on hydrogen transport in nanopolycrystalline
[9] ASTM International (2011). Standard practice for evaluation of hydrogen uptake, permeation, and transport in metals by an electrochemical technique. G148 − 97

APPENDIX

Appendix A: Derivation of Solution

$$\frac{\partial^2 c}{\partial x^2}+\frac{\partial^2 c}{\partial y^2}=\frac{1}{D}\frac{\partial c}{\partial \mathrm{t}}$$

Solution of SLP for X-Boundary Conditions: Neuman – Dirichlet

$$\lambda_n=\left(n+\frac{1}{2}\right)\frac{\pi}{L}$$

$$X_n(x)=\cos(\lambda_n x)$$

$$\|X_n(x)\|^2=\frac{L}{2}$$

$$F_x\left\{\frac{\partial^2 c}{\partial x^2}\right\}=-\lambda_n^2\overline{c_n}-f_0X_n(0)-f_LX_n{}'(L)$$

where $f_0=f(0,y,t)$ and $f_L=0$

Solution of SLP for y-Boundary Conditions: Dirichlet -- Dirichlet

$$\mu_m=\frac{m\pi}{L}$$

$$Y_m(y)=\sin(\mu_m y)$$

$$\|Y_m(y)\|^2=\frac{M}{2}$$

$$F_y\left\{\frac{\partial^2 c}{\partial y^2}\right\}=-\mu_m^2\overline{c_m}+f_0Y_m(y)-f_LY_m{}'(M)$$

where $f_0=f_L=0$

Applying the Finite Fourier Transform to Fick's Law:

$$F_x\left\{F_y\left\{\frac{\partial^2 c}{\partial x^2}+\frac{\partial^2 c}{\partial y^2}=\frac{1}{D}\frac{\partial c}{\partial \mathrm{t}}\right\}\right\}=F_x\left\{F_y\left\{\frac{1}{D}\frac{\partial c}{\partial \mathrm{t}}\right\}\right\}$$

$$-\lambda_n^2\bar{c}_{nm}-f_0X_n(0)-\mu_m^2\bar{c}_{nm}=\frac{1}{D}\frac{\partial}{\partial t}\bar{c}_{nm}$$

where $\bar{c}_{nm}=F_x\{F_y\{c(x,y,t)\}\}$

Applying the Laplace Transform:

$$\mathcal{L}\{-\lambda_n^2\bar{c}_{nm}-f_0X_n(x)-\mu_m^2\bar{c}_{nm}\}=\mathcal{L}\left\{\frac{1}{D}\frac{\partial}{\partial t}\bar{c}_{nm}\right\}$$

$$-\lambda_n^2C_{nm}-\mathcal{L}\{f_0X_n(0)\}-\mu_m^2C_{nm}=\frac{s}{D}C_{nm}$$

where $C_{nm}=\mathcal{L}\{\overline{c_{nm}}\}$

Organizing Terms:

$$C_{nm}\left(\frac{s}{D}+\lambda_n^2+\mu_m^2\right)=-\mathcal{L}\{f_0X_n(0)\}$$

$$C_{nm}=-\frac{1}{\frac{s}{D}+\lambda_n^2+\mu_m^2}\mathcal{L}\{f_0X_n(0)\}$$

$$C_{nm}=-\frac{D}{s-\left(-D(\lambda_n^2+\mu_m^2)\right)}\mathcal{L}\{f_0X_n(0)\}$$

where $\mathcal{L}\left\{e^{-D(\lambda_n^2+\mu_m^2)t}\right\}=\frac{1}{s-\left(-D(\lambda_n^2+\mu_m^2)\right)}$

Take the Inverse Laplace Transform using the Convolution Integral:

$$\mathcal{L}^{-1}\{C_{nm}\}=\mathcal{L}^{-1}\left\{-\frac{D}{s-\left(-D(\lambda_n^2+\mu_m^2)\right)}\mathcal{L}\{f_0X_n(0)\}\right\}$$

$$\bar{c}_{nm}=-D\left(e^{-D(\lambda_n^2+\mu_m^2)t}*f_0X_n(0)\right)$$

$$\bar{c}_{nm}=-D\int_{\tau=0}^{\infty}e^{D(\lambda_n^2+\mu_m^2)(\tau-t)}f_0X_n(0)\,d\tau$$

where $X_n(0) = 1$

$$\bar{c}_{nm} = -D \int_{\tau=0}^{\infty} f_0 e^{D\left(\lambda_n^2+\mu_m^2\right)(\tau-t)}\, d\tau$$

Solution of the Finite Fourier Transform:

$$c(x,y,t) = \sum_{n=1}^{\infty}\sum_{m=1}^{\infty} \bar{c}_{nm} \frac{X_n(x)}{\|X_n(x)\|^2}\frac{Y_m(y)}{\|Y_m(y)\|^2}$$

$$c(x,y,t) = \frac{4D}{LM}\sum_{n=1}^{\infty}\sum_{m=1}^{\infty} \bar{c}_{nm}\cos(\lambda_n x)\sin(\mu_m y)$$

